EXACT MAXIMUM LIKELIHOOD TIME DELAY ESTIMATION

Benoit Champagne, Moshe Elzenman and
Subbarayan Pasupathy

Department of Electrical Engineering, University of Toronto
Toronto, Ontario, Canada, M5S 1A4

ABSTRACT

This paper presents an exact solution to the problem of maximum likelihood time delay estimation over arbitrary observation time T. That is, the standard assumption $T \gg \tau_c + d_{max}$ made in the derivation of the asymptotic maximum likelihood (AML) estimator, where τ_c is the correlation time of the various processes involved and d_{max} the maximum permissible delay, is relaxed. The exact maximum likelihood (EML) processor is shown to consist of a special finite time beamformer, followed by a scalar postprocessor based on the eigenvalues and eigenfunctions of a certain integral equation. The solution of this integral equation is obtained for the case of stationary signals with rational power spectral densities (PSD). The performances of EML and AML are compared by means of computer simulations for a first order low-pass PSD. The results show that EML can lead to a significant improvement in performances (bias, variance, large errors) when the condition $T \gg \tau_c + d_{max}$ is not satisfied.

I. INTRODUCTION

In [1], the asymptotic maximum likelihood (AML) time delay estimator is derived under the assumptions that the signal and noise statistics are stationary and that the condition $T \gg \tau_c + d_{max}$ is satisfied, where T is the length of the observation interval, τ_c is the maximum correlation time of the random processes involved, and d_{max} is the maximum permissible delay. In many practical applications of time delay estimation (TDE), however, the signal and noise statistics and, more importantly, the time delay itself, can not be considered stationary unless small observation times T are used. In other applications, the length of the data set available may simply be insufficient for the condition $T \gg \tau_c + d_{max}$ to be satisfied. These considerations justify the need for new TDE techniques that can be used over arbitrarily small observation intervals.

In this paper, we present an exact analytical solution to the problem of maximum likelihood TDE which is valid for arbitrary observation times T. By means of computer simulations, we also compare the performances of the resulting exact maximum likelihood (EML) estimator to those of the AML estimator.

II. PROBLEM FORMULATION

We consider the family of vector random processes $\mathbf{x}(t;d)$, parametrized by the delay variable $d \in [-d_{max}, d_{max}]$, and defined as follows:

$$\mathbf{x}(t;d) = \mathbf{a}(t;d) + \mathbf{n}(t), \quad 0 \le t \le T, \tag{1}$$

$$\mathbf{a}(t;d) = \begin{bmatrix} a(t) \\ a(t-d) \end{bmatrix}, \quad \mathbf{n}(t) = \begin{bmatrix} n_1(t) \\ n_2(t) \end{bmatrix}, \tag{2}$$

where the signal component $a(t)$ and the additive noise components $n_i(t)$, $i=1,2$, are zero mean, uncorrelated, stationary Gaussian random processes with autocorrelation $R_a(\tau)$ and $R_{n_i}(\tau)$, respectively. We assume that the power spectral density (PSD) of the process $a(t)$, defined as

$$G_a(\omega) = \int_{-\infty}^{\infty} R_a(\tau)\, e^{-j\omega\tau}\, d\tau, \tag{3}$$

takes the irreducible form

$$G_a(\omega) = \frac{N(s^2)}{D(s^2)}, \quad s = j\omega, \tag{4}$$

where $N(.)$ and $D(.)$ are real coefficient polynomials of degree m and n respectively, satisfying the following conditions: (a) $N(s^2)$ can only have $j\omega$–axis zeros of even multiplicities; (b) $D(s^2)$ has no $j\omega$–axis zero and; (c) $n \ge m+1$. We further assume that the additive noise components $n_i(t)$ are white, that is,

$$R_{n_i}(\tau) = \frac{N_0}{2}\,\delta(\tau), \tag{5}$$

where $\frac{N_0}{2} > 0$ represents the noise power level in the individual components of $\mathbf{x}(t;d)$.

Given an observation (i.e. a particular realization) $\mathbf{x}(t)$, $0 \le t \le T$, of the process $\mathbf{x}(t;d^*)$, where d^* represents the true value of the unknown delay parameter, the TDE problem consists in finding an estimate of d^* which is optimal in some statistical sense. One such estimate is the maximum likelihood (ML) estimate.

By definition, the ML estimate $\hat{d}_{ML}$ of d^* is the value of d at which the log-likelihood function $\ln \Lambda(\mathbf{x};d)$ attains a maximum, i.e.,

$$\hat{d}_{ML} = \arg\max \{\ln \Lambda(\mathbf{x};d) : -d_{max} \le d \le d_{max}\}. \tag{6}$$

The log-likelihood function admits the following series representation:

$$\ln \Lambda(\mathbf{x};d) = l_1(\mathbf{x};d) + l_2(d), \tag{7}$$

$$l_1(\mathbf{x};d) = \frac{1}{N_0} \sum_{i=1}^{\infty} \frac{\lambda_i(d)}{\lambda_i(d) + N_0/2} \left[\int_0^T \Phi_i^T(t;d)\, \mathbf{x}(t)\, dt \right]^2, \tag{8}$$

$$l_2(d) = \frac{-1}{2} \sum_{i=1}^{\infty} \ln[1 + 2\lambda_i(d)/N_0]. \tag{9}$$

The superscript ^{T} in (8) denotes transposition. $\lambda_i(d)$ and $\Phi_i(t;d)$ are the eigenvalues and normalized vector eigenfunctions, respectively, associated with the autocorrelation $R_{\mathbf{a}}(\tau;d)$ of the process $\mathbf{a}(t;d)$. In the general case, these eigenvalues and eigenfunctions will depend upon the parameter d. However, in order to simplify the notations, we shall subsequently omit this dependence. The determination of the λ_i and $\Phi_i(t)$ is the subject of the next two sections.

III. DIMENSIONALITY REDUCTION

Rather than considering the matrix integral equation that defines the λ_i and $\Phi_i(t)$ directly, we apply the technique of dimensionality reduction developed in [2]. This technique can be thought of as a generalization of the material presented in [3]. Its advantages are twofold. First, it permits us to obtain the $\Phi_i(t)$ by applying a simple linear transformation to the properly normalized eigenfunctions of a scalar integral equation whose eigenvalues are precisely the λ_i. Since solving a scalar integral equation is conceptually simpler than solving a matrix integral equation, this property in itself is very important. Second, the technique of dimensionality reduction provides information regarding the structure of the optimum processor specified by (7). More precisely, it decomposes

CH2673-2/89/0000-2633 $1.00

this processor into a generalized beamformer followed by a scalar post-processor.

For the case $0 < d < T$, the technique of dimensionality reduction yields the following results: Define the step function

$$\rho(t) = \begin{cases} 1 & \text{if } -d < t < 0 \\ 2 & \text{if } 0 < t < T-d \\ 1 & \text{if } T-d < t < T \end{cases} \tag{10}$$

and let λ_i and $\psi_i(t)$ be the eigenvalues and eigenfunctions of the scalar integral equation

$$\int_{-d}^{T} R_a(t-u)\,\psi_i(u)\,\rho(u)\,du = \lambda_i\,\psi_i(t), \quad -d \le t \le T, \tag{11}$$

with the $\psi_i(t)$ satisfying the orthonormality condition

$$\int_{-d}^{T} \psi_i(t)\,\psi_j(t)\,\rho(t)\,dt = \delta_{ij}. \tag{12}$$

Then, the functions

$$\Phi_i(t) = \begin{bmatrix} \psi_i(t) \\ \psi_i(t-d) \end{bmatrix}, \quad 0 \le t \le T. \tag{13}$$

are the normalized eigenfunctions of $R_{\mathbf{a}}(\tau;d)$ with eigenvalues λ_i. For the cases $d > T$ and $d < 0$, the technique of dimensionality reduction yields similar results, i.e., the eigenfunctions $\Phi_i(t)$ are given by (13) with λ_i and $\psi_i(t)$ satisfying integral equations similar to (11) and (12), the only difference being in the step function $\rho(t)$. In the case $d < 0$, there is no need to consider these modified integral equations since the following relations can be used directly (the dependence upon d has been reintroduced temporarily),

$$\lambda_i(d) = \lambda_i(|d|), \tag{14}$$

$$\psi_i(t;d) = \psi_i(t-|d|;|d|), \quad 0 \le t \le T+|d|. \tag{15}$$

In the remainder of this paper, we consider only the case $0 < d < T$.

We now look at the processor configuration that results from the specific structure of the eigenfunctions $\Phi_i(t)$. Making the substitution (13) in (7), we find that

$$l_1(\mathbf{x};d) = \frac{1}{N_0} \sum_{i=1}^{\infty} \frac{\lambda_i}{\lambda_i + N_0/2}\, y_i^2, \tag{16}$$

$$y_i = \int_{-d}^{T} \psi_i(t)\,y(t)\,dt, \tag{17}$$

where the scalar process $y(t)$ is given in terms of the components $x_1(t)$ and $x_2(t)$ of $\mathbf{x}(t)$ by

$$y(t) = \begin{cases} x_2(t+d) & \text{if } -d < t < 0 \\ x_1(t) + x_2(t+d) & \text{if } 0 < t < T-d \\ x_1(t) & \text{if } T-d < t < T \end{cases} \tag{18}$$

The resulting processor configuration is shown in Figure 1. It consists of a special finite time beamformer, whose action is specified by (18), followed by a scalar post-processor based on the λ_i and $\psi_i(t)$. A number of important observations can be made regarding the finite time beamforming operation (18). First, it features discontinuities at $t=0$ and $t=T-d$. These discontinuities, which we refer to as edge effects, result from the fact that the observation interval $[0,T]$ is finite. Second, the middle term on the right hand side of (18), which becomes the dominant term when $T \gg d$, corresponds to a simple, coherent, delay and sum beamforming operation. Finally, the operation (18) is robust in the sense that it is independent of the signal statistics. The scalar post-processor performs the operations specified by (16) and (17) on the output $y(t)$ of the finite time beamformer. In practice, only a finite number N of terms is included in (16).

IV. SOLUTION OF THE REDUCED INTEGRAL EQUATION

In this Section, we present an explicit operational solution algorithm for the reduced integral equation (11) which is applicable to stationary signal processes $a(t)$ with rational PSD's. Before we begin, it is important to understand that previous techniques available for the determination of the eigenvalues and eigenfunctions associated with the autocorrelation $R_a(\tau)$ of such processes do not apply in this case because of the non-constant step function $\rho(t)$ in equation (11). Moreover, because the off-diagonal elements of the matrix PSD $G_{\mathbf{a}}(\omega;d)$ of the process $\mathbf{a}(t;d)$ contain exponential factors of the type $e^{\pm j\omega d}$, neither it is possible to solve the matrix integral equation specifying the λ_i and $\Phi_i(t)$ directly by a straightforward multidimensional extention of the techniques already available. The novelty in the algorithm presented below is that it can deal with the non-constant step function $\rho(t)$ defined in (10). In fact, it could easily be extended to arbitrary finite step functions that are symmetric with respect to the middle point of their interval of definition.

In order to facilitate the understanding of the solution algorithm for equation (11), we begin by stating three simple but important properties that are satisfied by the eigenvalues and eigenfunctions of this equation.

Property 1. The eigenvalues λ_i are bounded. More precisely, $0 < \lambda_i < \gamma$, where

$$\gamma = 2 \max\{G_a(\omega): -\infty < \omega < \infty\}. \tag{19}$$

Property 2. The eigenfunctions $\psi_i(t)$ are continuous on the interval $[-d,T]$.

Property 3. There exists a complete orthonormal (in the sense of (12)) set of eigenfunctions $\{\psi_i(.)\}$, such that each eigenfunction in the set satisfies the symmetry relation

$$\psi_i(t) = \varepsilon_i\,\psi_i(T-d-t), \tag{20}$$

where ε_i, referred to as the symmetry index, is either equal to +1 or to −1.

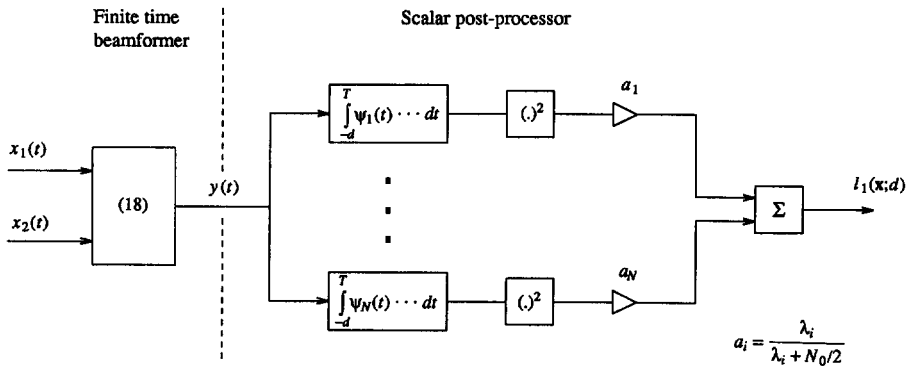

Figure 1. Configuration of the EML processor

Our solution algorithm for equation (11) generalizes Youla's technique [4] for the determination of the eigenvalues and eigenfunctions of $R_a(\tau)$ in the absence of the step function $\rho(t)$. Besides the various modifications that need to be made in order to account for this non-constant step function, there is one major distinction between our approach and Youla's approach that deserves some explanations. What makes Youla's technique efficient is the use of a symmetry argument that reduces by half the number of some unknown eigenfunction coefficients. In the original paper [4], indeed, it is shown, under certain simplifying assumptions, that the eigenfunctions of $R_a(\tau)$ must satisfy a symmetry relation which is the Laplace domain equivalent of (20) for $d=0$. Rather than making unnecessary simplifying assumptions, we have chosen a different approach: since Property 3 (whose proof does not rely on any supplementary assumption) asserts the existence of eigenfunctions satisfying the symmetry relation (20), we developed our solution algorithm so that it give precisely these eigenfunctions.

We now describe the various steps in our solution algorithm for equation (11):

(1) Determine the canonical factors $D^+(s)$ and $D^-(s)$ of $D(s^2)$ as follows,

$$D(s^2)=D^+(s)D^-(s),$$
$$D^-(s)=D^+(-s), \tag{21}$$
$$D^+(s) \text{ has only left-half-plane zeros.}$$

(2) Find the K_1 distinct roots $s_{1k}(\lambda)$, $k=1,...,K_1$, of the polynomial $\lambda D(s^2)-N(s^2)$ and let m_{1k} denote their respective multiplicities. Similarly, find the K_2 distinct roots $s_{2k}(\lambda)$, $k=1,...,K_2$, of the polynomial $\lambda D(s^2)-2N(s^2)$ and let m_{2k} denote their respective multiplicities. Observe that the zero configurations of both these polynomials are symmetric about the real axis and the $j\omega$-axis.

(3) Define the functions

$$g_1(s)=e^{sd}D^+(s)P(s)-Q(s), \tag{22}$$
$$g_2(s,\varepsilon)=Q(s)+\varepsilon e^{-s(T-d)}Q(-s), \tag{23}$$

where $\varepsilon=\pm 1$ and where $P(s)$ and $Q(s)$ are yet undetermined real coeficient polynomials of degrees $n-1$ and $2m-1$, respectively, i.e.,

$$P(s)=p_0+p_1 s+\cdots+p_{n-1}s^{n-1} \tag{24}$$
$$Q(s)=q_0+q_1 s+\cdots+q_{2n-1}s^{2n-1}. \tag{25}$$

(4) Consider the following system of $4n$ complex linear equations in the $3n$ real unknown coefficients $p_0,...,p_{n-1},q_0,\ldots,q_{2n-1}$,

$$g_1^{(l)}(s_{1k}(\lambda))=0, \quad l=0,...,m_{1k}-1, \quad k=1,...,K_1, \tag{26}$$
$$g_2^{(l)}(s_{2k}(\lambda),\varepsilon)=0, \quad l=0,...,m_{2k}-1, \quad k=1,...,K_2, \tag{27}$$

where the superscript (l) denotes the l^{th} derivative with respect to s.

(5)Using the symmetries present in the zero configurations $\{s_{1k}(\lambda)\}$ and $\{s_{2k}(\lambda)\}$ and in the functions $g_1(s)$ and $g_2(s,\varepsilon)$, transform this system into an equivalent system consisting of $3n$ real linear equations in the unknown $p_0,...,q_{2n-1}$. Let this new system be represented by the matrix equation

$$A(\lambda,\varepsilon)X=0 \tag{28}$$

where $A(\lambda,\varepsilon)$ is a $3n\times 3n$ real matrix and $X=[p_0,\ldots,q_{2n-1}]^T$.

(6) Find the roots $(\lambda_i,\varepsilon_i)$, with $0<\lambda_i<\gamma$ and $\varepsilon_i=\pm 1$, of the equation

$$\det A(\lambda,\varepsilon)=0. \tag{29}$$

The λ_i so obtained are the eigenvalues of equation (11) and the ε_i are the symmetry indices of the corresponding eigenfunctions.

(7) For each pair $(\lambda_i,\varepsilon_i)$, determine the solution space of the equation

$$A(\lambda_i,\varepsilon_i)X=0. \tag{30}$$

For simplicity, assume that the solution space has dimension one (the general case needs only minor modifications) and let $X_i=[p_{0,i},\ldots,q_{2n-1,i}]^T$ be an arbitrary non-zero element of the solution space.

(8) Let

$$P_i(s)=p_{0,i}+\cdots+p_{n-1,i}s^{n-1}, \tag{31}$$
$$Q_i(s)=q_{0,i}+\cdots+q_{2n-1,i}s^{2n-1}. \tag{32}$$

Then, we have

$$\psi_i(t)=\begin{cases} c_i\sum_{k=1}^{K_1}\text{Res}\left[\dfrac{D^+(s)P_i(s)e^{s(t+d)}}{\lambda_i D(s^2)-N(s^2)},s_{1k}(\lambda_i)\right], & -d<t<0 \\ c_i\sum_{k=1}^{K_2}\text{Res}\left[\dfrac{Q_i(s)e^{st}}{\lambda_i D(s^2)-2N(s^2)},s_{2k}(\lambda_i)\right], & 0<t<T-d \end{cases} \tag{33}$$

where c_i is a (yet undetermined) coefficient and where the notation $\text{Res}[f(s),s_0]$ is used to denote the residue of the function $f(s)$ at one of its pole s_0. For $T-d<t<T$, $\psi_i(t)$ can be obtained from (33) by making use of the symmetry relation (20).

(9) In order to determine c_i, simply substitute the above expressions for $\psi_i(t)$ into (12) and perform the appropriate integration.

This completes the algorithm.

V. COMPUTER SIMULATIONS

In this Section, computer simulations are used to study the comparative performance of EML and AML for a low-pass first order PSD $G_a(\omega)$. Our principal objective here is not to provide the reader with an exhaustive study, but rather to show that in some particular cases where the condition $T\gg\tau_c+d_{\max}$ is violated, EML can outperform AML in a significant way. Accordingly, only a few values of the parameters of interest, i.e, bandwidth, delay and signal-to-noise ratio, are considered. We begin by briefly describing the simulations and then follow with a discussion of the results.

The signal $a(t)$ was modeled as a first order stationary Markov process with autocorrelation

$$R_a(\tau)=P e^{-\alpha|\tau|}, \quad P,\alpha>0, \tag{34}$$

and corresponding PSD

$$G_a(\omega)=\frac{2\alpha P}{\omega^2+\alpha^2}. \tag{35}$$

P is the mean square value of the signal $a(t)$ and α is the inverse of its correlation time, simply defined as the $1/e$ point of $R_a(\tau)$. α also gives the -3dB point of $G_a(\omega)$, so we refer to the quantity αT as the time bandwidth product. Furthermore, it is convenient to define the signal-to-noise ratio (SNR) as the total signal energy per channel divided by the noise power level, i.e.,

$$\text{SNR}=\frac{PT}{(N_0/2)}. \tag{36}$$

The EML estimate $\hat{d}_{\text{EML}}$ was obtained by maximizing the log-likelihood function (7) over a restricted set of delay values. The processor of Figure 1, with $N=3\alpha T$, was used to compute the data dependent term $l_1(\mathbf{x};d)$ in (7). The bias term $l_2(d)$ was precomputed. For the search of the maximum, a grid of 21 equally spaced delay values centered at d^* was used, i.e.,

$$d=kT_s, \quad k\in\{k^*-10,...,k^*+10\}. \tag{37}$$

Here, T_s is the sampling interval of the grid and $k^*=d^*/T_s$ is the true value of the delay parameter in samples. For the simulations considered, the choice $T_s=1/(10\alpha)$ provided sufficient resolution in the delay estimate. After the value of d maximizing the log-likelihood function had been found, a three point quadratic interpolation formula was used to determine d_{EML}.

Similarly, the AML estimate $\hat{d}_{\text{AML}}$ was obtained by maximizing the asymptotic log-likelihood function

$$L(\mathbf{x};d)=\frac{2}{N_0}\sum_{i=1}^{M}\frac{2G_a(\omega_i)}{2G_a(\omega_i)+N_0/2}|X_i|^2, \quad \omega_i=\frac{2\pi i}{T}, \tag{38}$$

$$X_i=[1,e^{j\omega d}]\frac{1}{\sqrt{2T}}\int_0^T \mathbf{x}(t)e^{-j\omega_i t}\,dt, \tag{39}$$

over the grid (37) and by applying the same interpolation formula as above. In order to make our comparison of EML and AML meaningful we chose $M=3\alpha T/2$ as the upper limit of summation in (38).

For the simulation, the following parameter values were used:

$$\alpha T = 4,$$
$$\text{SNR} = 125, 500, \tag{40}$$
$$k^* = 0, 4, 8, 12, 16.$$

For each choice of k^* and SNR, 256 independent experiments were run, and at the end, the various performance indicators were computed for both EML and AML. The indicators considered were the bias, the standard deviation, and the number of delay estimates falling on the boundaries $(k^* \pm 10)T_s$. They are represented here by β, σ, and η, respectively. σ was used as a measure of small errors while η was used as a very crude measure of large errors. The results of these simulations are presented in Table 1, 2 and 3.

True delay k^* (samples)	Bias (samples)			
	SNR=125		SNR=500	
	β_{EML}	β_{AML}	β_{EML}	β_{AML}
0	-0.00	-0.03	-0.03	-0.04
4	-0.00	-0.53	0.00	-0.49
8	0.08	-0.94	0.04	-0.89
12	0.13	-1.68	0.06	-1.77
16	0.22	-1.31	0.04	-1.09

Table 1. Comparison of bias for EML and AML

True delay k^* (samples)	Standard deviation (samples)			
	SNR=125		SNR=500	
	σ_{EML}	σ_{AML}	σ_{EML}	σ_{AML}
0	1.15	1.31	0.33	1.03
4	0.81	1.75	0.33	1.39
8	0.84	2.84	0.36	2.25
12	1.45	4.73	0.48	4.51
16	1.88	5.42	0.84	5.42

Table 2. Comparison of standard deviation for EML and AML

True delay k^* (samples)	Number of boundary estimates			
	SNR=125		SNR=500	
	η_{EML}	η_{AML}	η_{EML}	η_{AML}
0	0	1	0	1
4	0	3	0	2
8	0	5	0	2
12	2	29	0	27
16	4	43	1	42

Table 3. Comparison of η_{EML} and η_{AML}

True delay k^* (samples)	Improvement factor IMP (bB)	
	SNR=125	SNR=500
0	1.1	9.9
4	6.7	12.5
8	10.6	15.9

Table 4. Improvement factor

From table 1, we observe that the EML estimate is practically unbiased. This property is not shared by the AML estimate. Indeed, AML introduces a negative bias which generally increases in magnitude with k^*. Moreover, the magnitude of this bias seems to be independent of the SNR.

We now consider Table 2. Our first observation is that for a fixed value of k^*, both σ_{EML} and σ_{AML} decrease as the SNR increases. However, this effect is much less pronounced for AML than it is for EML. Second, we note that both σ_{EML} and σ_{AML} increase with k^* (the only exception to this rule being with σ_{EML} for SNR=125 and k^*=4,8). This result is understandable since, as k^* increases, the edge effects become more important and only a smaller portion of the signal $x_1(t)$ and $x_2(t)$ can be processed coherently. In order to compare σ_{EML} with σ_{AML}, we define an improvement factor as follows,

$$\text{IMP} = 20 \log \frac{\sigma_{AML}}{\sigma_{EML}}. \tag{41}$$

Computed values of IMP for k^*=0,4,8 have been collected together in Table 4. We note that for the simulation experiments considered, IMP is always positive and is an increasing function of both k^* and the SNR. As seen from the table, significant performance improvements can be obtained by using EML instead of AML. Finally, it is important to notice the large increase in σ_{AML} that occurs between k^*=8 and k^*=12. In fact, for $k^* \geq 12$, σ_{AML} comes very close to the limiting value of 5.77, which is the standard deviation for delay estimates uniformly distributed in the window $[k^*-10, k^*+10]$. Hence, for k^* larger than 8 (this represents 20% of the total observation time), AML is unreliable and should not be used, at least for the particular PSD considered in these simulations.

The fact that AML becomes unreliable somewhere between k^*=8 and k^*=12 is also confirmed by the results of Table 3. As can be seen from this Table, η_{AML} increases from a few units at k^*=8 to around 30 at k^*=12. What is even worst for the AML estimate is that this threshold effect does not seem to disappear as the SNR increases. In the case of EML, however, no such undesirable threshold effects occur.

VI. CONCLUSIONS

The main results of this work are summarized below:

(a) A new processor configuration was obtained for the problem of ML TDE over arbitrary observation time. This configuration consists of a finite time beamformer followed by a scalar post-processor whose implementation requires the knowledge of the eigenvalues and eigenfunctions of a certain integral equation.

(b) An explicit operational solution algorithm for this integral equation that applies to stationary signals with rational PSD's was developed.

(c) Computer simulations were used to compare the performances of EML and AML in a few particular cases. They show that EML can lead to a significant improvement in the performances (bias, variance, large errors) when the condition $T \gg \tau_c + d_{max}$ is not satisfied.

VII. REFERENCES

[1] C.H. Knapp and G.C. Carter, "The generalized correlation method for estimation of time delay", IEEE Trans. Acoust., Speech, Signal Processing, vol. ASSP-24, no. 4, pp. 320-327, 1976.

[2] B.Champagne, M. Eizenman, and S. Pasupathy, "A dimensionality reduction technique for optimum array processing of non-stationary signals", under preparation.

[3] J.A. Stuller, "Maximum-likelihood estimation of time-varying delay - Part I", IEEE Trans. Acoust., Speech, Signal processing, vol. ASSP-35, no. 3, pp 300-313, 1987.

[4] D.C. Youla, "The solution of a homogeneous Wiener-Hopf integral equation occuring in the expansion of second-order stationary random functions", IRE Trans. Inform. Theory, vol. IT-3, pp. 187-193, 1957.